


## ORIGINAL RESEARCH

# Integration of close-range underwater photogrammetry with inspection and mesh processing software: a novel approach for quantifying ecological dynamics of temperate biogenic reefs

Daniele Ventura<sup>1</sup> , Stanislas F. Dubois<sup>2</sup>, Andrea Bonifazi<sup>3</sup>, Giovanna Jona Lasinio<sup>4</sup>, Marco Seminara<sup>1</sup>, Maria F. Gravina<sup>3,4,5</sup> & Giandomenico Ardizzone<sup>1</sup>

<sup>1</sup>Department of Environmental Biology, University of Rome "la Sapienza", V. le dell'Università 32, Rome 00185, Italy

<sup>2</sup>IFREMER, DYNECO-LEBCO, Centre de Bretagne, Technopole Brest-Iroise, 1625 route de Sainte-Anne, CS 10070, Plouzané 29280, France

<sup>3</sup>Laboratory of Experimental Ecology and Aquaculture, Tor Vergata University, Via della Ricerca Scientifica, Rome 00133, Italy

<sup>4</sup>Department of Statistic, Sciences, University of Rome "la Sapienza" - V. le dell'Università 32, Rome 00185, Italy

<sup>5</sup>CoNISMa, Consorzio Nazionale Interuniversitario per le Scienze del Mare, Rome, Italy

## Keywords

3D modelling, biogenic temperate reefs, computer vision, mesh analysis, surface rugosity evaluation, volumetric estimates

## Correspondence

Daniele Ventura, Department of Environmental Biology, University of Rome "la Sapienza", V. le dell'Università 32, 00185 Rome, Italy. Tel: +39-3337632025; Fax: 06 4991 2436-2561-2435; E-mail: daniele.ventura@uniroma1.it.

Editor: Kylie Scales

Associate Editor: Gwilym Rowlands

Received: 18 March 2020; Revised: 27 July 2020; Accepted: 6 August 2020

doi: 10.1002/rse2.178

## Abstract

Characterizing and monitoring changes in biogenic 3-dimensional (3D) structures at multiple scales over time is challenging within the practical constraints of conventional ecological tools. Therefore, we developed a structure-from-motion (SfM)-based photogrammetry method, coupled with inspection and mesh processing software, to estimate important ecological parameters of underwater worm colonies (hummocks) constructed by the sabellariid polychaete *Sabellaria alveolata*, using non-destructive, 3D modeling and mesh analysis. High resolution digital images of bioconstructions (hummocks) were taken *in situ* under natural conditions to generate digital 3D models over different sampling periods to analyse the morphological evolution of four targeted hummocks. 3D models were analysed in GOM Inspect software, a powerful and freely available mesh processing software to follow growth as well as morphology changes over time of each hummock. Linear regressions showed 3D models only slightly overestimated the real dimensions of the reference objects with an average error < 5% between measured and model-estimated dimensions for both length and volume. Manual inspection of models and semi-automated surface-to-surface comparison allowed the computation of important metrics linked to the ecology of temperate reefs such as volume, surface area, surface complexity/rugosity, number and size of holes and creeks and the mean density of living worms per colony. Moreover we demonstrated the reliability of 3D surface complexity estimates against two linear rugosity measures: a traditional and a virtual variant of the 'chain-and-tape' method. Finally, besides 3D models deviation analysis via surface comparison, a Bayesian latent variable model approach was adopted to highlight the significative effects of sea state conditions on *S. alveolata* hummocks metrics. We demonstrated without damaging the benthic organisms that SfM approach allow continuous study of temperate bioconstruction leading to a fine description of short-term structural modification mediated by hydrodynamics, making this technique accessible and repeatable to many other areas of ecological research.

## Introduction and Background

The term ‘ecosystem engineer’ refers to organisms that indirectly or directly modulate the availability of resources to other species via structural modifications of the environment (Lawton and Jones, 1995; Bruschetti 2019). Biogenic structures built by a wide diversity of ecosystem engineers such as corals, bryozoans, bivalves or polychaetes provide key ecological functions in systems where they develop, such as habitat provision, nursery, feeding ground or protection against coastal erosion to cite a few examples (Goldberg 2013). In temperate regions, large bioconstructions are built by polychaetes of the family Sabellariidae. The honeycomb worm *Sabellaria alveolata* (Linnaeus, 1767) is a filter-feeding gregarious tubicolous species that builds wave-resistant reefs by transforming soft-sedimentary habitats into engineered hard bioconstructions in intertidal areas (Jones et al. 2018; Curd et al. 2019). Worms selectively used mineral sand grains and shell debris (between 63 µm and 2 mm on the Wentworth Scale) glued with organic cement (Naylor and Viles, 2000) to construct their tubes. Bioconstructions are widespread along European Atlantic coasts, occurring on intertidal shores from the Solway Firth (West Scotland) to the south of Morocco (Dubois et al. 2007), where they can exhibit a wide diversity of types and phases (see Fig. 1). In Curd et al. (2019), from veneers in the meter-square range encrusting rocky shores to very large platforms covering hectares in soft-sediment. *S. alveolata* is considered as the most important building organism in European temperate shallow environments, and has built to date the largest European animal construction (Dubois et al. 2002; Desroy et al. 2011). Previous investigations revealed that they engineer biotopes of great biological conservation value with high species richness (biodiversity hotspots) (Dubois et al. 2002). *S. alveolata* reefs play also key ecological roles in ecosystems, such as biological filters (Dubois et al. 2009), sediment stabilizer and bioclasts trappers (Desroy et al. 2011). They also bear high aesthetic or recreational value (Dubois et al. 2006). For these reasons, these reefs are listed under Annex I of the EC Habitats Directive (Council Directive EEC/92/43 on the Conservation of Natural Habitats and of Wild Fauna and Flora) as a marine habitat to be protected by the designation ‘Special Areas of Conservation’.

Intertidal and shallow water biogenic reefs are highly affected by physical perturbations such as natural events (storms, river runoffs) and anthropogenic pressures, either directly (boat anchoring and trampling), or indirectly such as aquaculture and fish farming (Dubois et al. 2002; Plicanti et al. 2016). Resistance and resilience of biogenic reefs are highly dependent of reproductive

outputs and juvenile’s settlement (Dubois et al. 2007; Ayata et al. 2009) but is also linked to the physical phase of the reef (Curd et al. 2019). Information on growth phase, morphological characteristics and structural complexity can be key elements to comprehensively assess biogenic reef dynamics and to evaluate health conditions of the bioconstructions (Rossi et al. 2019). Several studies of coral reefs demonstrated that structural complexity correlates strongly with indicators of reef health and biodiversity metrics associated to the habitat (McCormick 1994; Young et al. 2017). More precisely rugosity and surface complexity of coral reefs relate directly on benthic current dynamics (Pittman and Brown, 2011) and are important predictors of organismal abundance and fish assemblages composition and ultimately reef functioning (House et al. 2018).

Usually, temperate and tropical biogenic reef metrics such as vertical relief, number of holes, surface complexity or rugosity, have been commonly estimated by direct *in situ* measures through SCUBA divers (Bamber and Irving, 1997; Harborne et al. 2012). Benthic survey protocols include intrusive methods that could damage colonies. For instance, *S. alveolata* reef thickness can be measured by scuba-divers equipped with a fine metric pole driven into the biogenic structure (Gravina et al. 2018). In coral reef environments, measurement of rugosity generally relied on the ‘chain-and-tape’ method, whereby the actual surface distance on the reef is measured by draping a chain over the substrate, and compared with a linear distance measured with a transect tape (McCormick 1994). While this technique is simple and inexpensive, the chain often tangle and possibly damage the reef, and is a labor-intensive and time-consuming task (Friedman et al. 2012; Burns et al. 2015). Moreover using a linear distance measure to describe 3D landscapes may led to large variation in the rugosity measure with only minor changes in chain placement (Friedman et al. 2012). Other common methods for measuring volume and surface area, such as water displacement (Cocito et al. 2003) and paraffin wax coating (Naumann et al. 2009), require removal – and most of the time destruction – of the benthic species from its natural environment.

Some recent studies originating from the fields of computer vision and photogrammetry aimed at defining physical and morphological reef features by applying non-intrusive techniques based on 3D modelling to measure volume, surface area and rugosity of corals (Lavy et al. 2015; Storlazzi et al. 2016; Gutierrez-Heredia et al. 2016; Raoult et al. 2017; Palma et al. 2017; Fukunaga et al. 2019). These approaches were limited to coral bioconstructions and developments to other biogenic structures such as sabellariid reefs are yet to be investigated (D’Urban Jackson et al. 2020). Over the past decade,

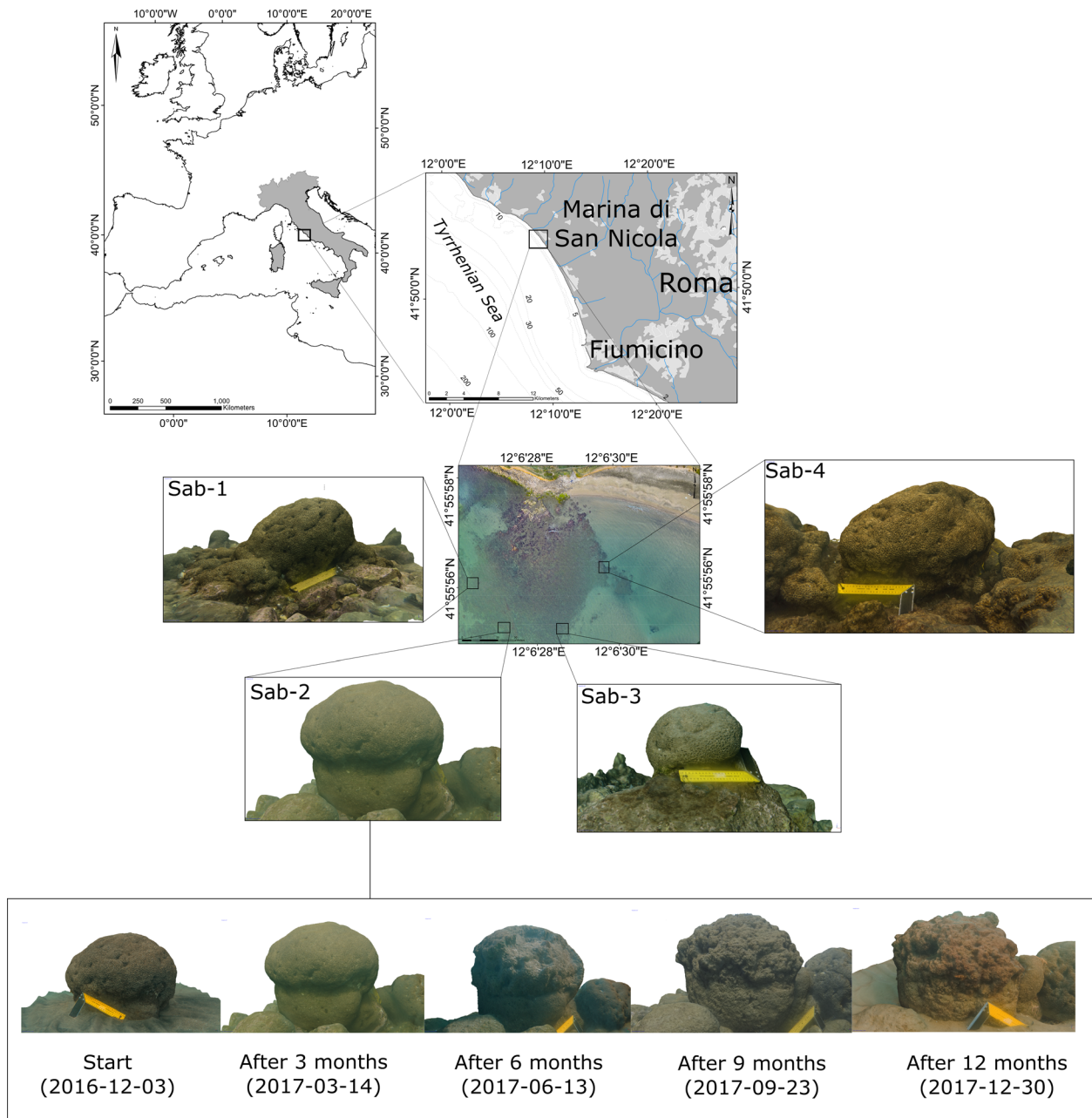


**Figure 1.** UAS-based orthophotos showing the geographical position (coordinates format on the margin of the maps are expressed in WGS 84 UTM 32 N) of the study site where the four bioconstructions of *Sabellaria alveolata* (from Sab-1 to Sab-4) were sampled through close-range structure from motion (SfM) underwater photogrammetry. In the bottom frame, an example of 3D textured meshes showing the temporal sequence of Sab-2 hummock over the whole sampling period (from 3 December 2016 to 31 December 2017). Other rendered models are reported in Figure S1.

advances in treatments of remote sensing data have allowed further characterization of *Sabellaria* reefs morphology. In particular, aerial data acquired from both multispectral (Collin et al. 2018; Collin et al. 2019) and three-band RGB cameras based on Structure from Motion (hereafter SfM) imagery (Ventura et al. 2018), LiDAR

(Light Detection and Ranging) systems (Noernberg et al. 2010) and high-frequency acoustic systems (Harrison et al. 2011) have been used for mapping emerging and submerged biogenic *Sabellaria* reefs and to make fine-scale measurements of bathymetry. These techniques have made possible to map large shallow areas efficiently at

depth resolutions of decimetres, but generally produces data at spatial resolutions on the order of meters (Storzazzi et al. 2016), which are often incompatible with small-scale assessments aimed at understanding 3D habitat complexity and short-term changes of the bio-constructive role of this species.

Considering these aspects, this study is the first attempt to determine whether close range SfM-based 3D photogrammetric modelling could reliably be used, in place of traditional methods, to measure important reef structural metrics such as volume, surface area and rugosity of *S. alveolata* colonies. Moreover we used 3D mesh processing software for a better understanding of morphological change over time of biogenic *Sabellaria* hummocks and to assess the effects of waves on this species that appears to play a considerable role for the ecology of the coastal systems. These approaches aiming at detecting fine changes in the morphology of hummocks coupled with environmental and physics data (e.g. sedimentation rates, nutrients input, waves and wind intensity, currents) provide a very flexible system which may increase the comprehension of reef development phases, leading to a higher probability of obtaining more effective management plans of biogenic formations along coastal habitats.

## Materials and Methods

### Underwater images acquisition

The study area (Fig. 1) was located along a sandy coast (Marina di San Nicola - 12°6'27.385"E; 41°55'55.647"N - Central Tyrrhenian Sea) exposed to southern winds, where *Sabellaria* bioconstructions are typified by large reef platforms as well as mosaic of hummocks and veneer reef types. In this area fine sand are the main substratum from 0 to 10 m depth, approximately 2 km away from the shoreline the sea bottom reaches a maximum depth of 20 m. At this depth, the sand is essentially replaced by fine-grained muddy sediments due to the proximity of Tiber river and some coralligenous outcrops are present.

To test if close-range SfM underwater photogrammetry could be used efficiently to depict the 3D changes in shape over time due to growth and latent hydrodynamics effects generated by waves, three isolated hummocks (ball-shaped colonies, hereafter referred to as Sab-1, Sab-2 and Sab-3) on sand and one coalescent hummock (hereafter referred to as Sab-4) inside a massive reef of *Sabellaria*, were photographed underwater (from 1 m to 3.5 m depth), approximately on a 3-monthly basis (according to sea conditions) from December 2016 to December 2017, over a 1-year study.

Each colony was photographed *in situ* using a Sony alpha 6000 (Sony Inc., New York, USA) digital APS-C

camera (CMOS 24 Megapixel sensor, sensor Size: 23.5 × 15.6 mm, pixel size: 3.92 μm) equipped with a 20 mm prime lens and a Meikon underwater housing with flat port. Natural lighting was used to reduce the effect of light changes in shadows. RAW format was adopted to allow for a more accurate post-processing of images. White balance was set to 6000K to suppress blue hues, shutter speed comprised between 1/80 and 1/200 and ISO lower than 1200. To ensure a sufficient depth of field, aperture was set at a f-stop of f/8-16. All acquisitions have been made at distance range between 0.5 and 1 meters with a GSD (Ground Sample Distance) in the range 0.3 and 0.8 mm. The environmental conditions of study site, specifically light availability due to water turbidity must be considered when selecting the camera settings as an improper depth of field and too high ISO values can dramatically influence the final resolution and precision of underwater photogrammetry (Burns et al. 2015). This species builds complex 3D structure and, therefore, presents a difficult object for accurate 3D reconstruction. Because turbidity may affect images acquisition, photographic surveys were carried out during low tide (to reduce the light attenuation due to the water column) and during calm sea states (no more than 0.40 cm wave height) to avoid fine sediment resuspension. As SfM requires a reference object with known dimensions to accurately scale and measure subjects, two 25 cm carpenter's squares were placed next to each surveyed hummock. From 80 to 250 (depending on hummock morphology and size) overlapping photographs were taken through two sets of full circles that allowed circular shooting (360°) around the target hummock, with slightly different trajectories and perspectives (20° to 45° angle, to provide more camera positions for 3D reconstruction and reduce occlusions). The main goal was to obtain at least 80% overlap between images which allowed good image alignment during SfM processing of images and to ensure high quality of the reconstructed point clouds (Raoult et al. 2016; Raoult et al. 2017).

### Weather data

Average daily values of sea weather conditions according to Douglas sea state (Fig. S2) was derived from hourly data from the near weather station of Civitavecchia monitored by the National Air Force Weather Data Center available at: <http://clima.meteoam.it/RicercaDati.php>.

### Image processing and 3D model generation

Prior to photogrammetry workflow, all images were manually enhanced. Minor adjustments regarding white

balance, color contrast and saturation, exposure, shadows/highlights were performed in Adobe Lightroom v. 5.1 (Adobe Systems, San Jose, CA, USA) to get more natural colors and defined edges. Subsequently chosen settings were applied to all images acquired the same day. Camera calibration, optimization, and 3D models of *Sabellaria* hummocks were computed using Agisoft PhotoScan Professional Edition V. 1.3.2 (Agisoft LLC, St. Petersburg, Russia). PhotoScan is a software for SfM photogrammetry which utilizes a sequence of overlapping digital images of a static subject taken from different spatial positions to produce a 3D point cloud by estimating 3D geometry of the scene and camera positions through bundle adjustment algorithm. The software can derive optical characteristics such as internal and external camera orientation parameters, including non-linear radial distortions directly from image's EXIF metadata, performing camera calibration using Brown's distortion model, eliminating the significant burden of pre-calibration (Burns et al. 2015). In fact, using the camera calibration parameters obtained from the self-calibration during the alignment stage, PhotoScan removes the lens distortion from the images for further processing. To allow the reconstruction of three-dimensional scene geometry, SfM algorithms detect image feature points and subsequently monitor the movement of those points throughout the sequence of multiple images; subsequently the locations of those feature points can be estimated and rendered as a sparse three-dimensional point cloud (Verhoeven 2011). Before aligning images loaded into PhotoScan, the software's 'Image Quality' tool was used to filter photos. Only photos reaching a quality threshold ( $>0.5$ , as measured by the software algorithms) were used to further processes. Underwater images of hummocks were rendered into 3D models at different sampling times (Fig. S1) following the standard procedures: (1) aligning photos, (2) marker-based optimization of camera position (3) building dense point cloud, (4) building 3D mesh, and (5) building texture. Digital markers were annotated onto the carpenter's squares, and the points were then used to create a scale bar set to the actual length of the square. The 3D point cloud of the *Sabellaria* hummocks was manually cropped from the rest of the scene to preserve only the living part of hummocks (with evident tube apertures). All processes were set to medium quality with default settings to obtain the best balance between processing time and model quality. The final rendered 3D models were then exported as a stereolithography (.STL file format). An ASUS mobile workstation G703 with 2.9 GHz Intel Core i7-7820HK (quad-core, RAM: 32GB; Graphics: Nvidia GeForce GTX 1080 8GB) was used to perform the analysis and the total processing time in PhotoScan lasted

approximately 2.5 h per hummock. A similar methodology was developed in previous studies designed to 3D-model coral reefs (Figueira et al. 2015; Ferrari et al. 2017; Fukunaga et al. 2019). All the steps used in this work are summarized in the workflow reported in Figure 2.

### 3D model analysis and measurement of hummocks' metrics

The scaled STL models were imported into GOM Inspect (GOM Inspect Version 10.1 2018; a free software from Gesellschaft für Optische Messtechnik, Braunschweig, Germany) to extract key reef metrics capable of describing the morphological changes of the hummocks over time. This 3D inspection and mesh processing software usually used in Computer Aided Design (CAD) modelling and engineering applications provides several functions for 3D model analysis, including mesh editing, volume and surface comparison of 3D objects, manual and semi-automatic with best-fit alignment.

Before performing measurements, refinement and cleaning of meshes were carried out with 'smooth' and 'refine' tools (available in mesh operation toolbox) to simplify the rough surfaces of hummocks and speed up the procedures. Even though these steps led to a mean loss of colony volume equal to  $-0.49\%$  ( $N = 4$ ,  $SE = 0.01$ ) they were necessary to standardize models (by removing surface roughness generated by sandy tubes), making more evident the morphology of *Sabellaria* bio-constructions (Fig. 3). In sabellariid reefs, not all tubes are occupied by a living worm. A small percentage of tube is actually empty or re-colonized by associated species (Bonifazi et al. 2019). Tubes with active individuals are characterized with large sandy porches – or apertures – cleared of epibionts (Curd et al. 2019). Prograding reefs showing growth extensions are then the result of worms with tube-building activity (la Porta and Nicoletti, 2009). The 3D surface areas with no living tubes (i.e. holes and crevices) were manually selected, then the number ( $N_{[holes]}$ ) and surface area ( $SA_{[holes]}$ ) were computed. The size of holes ( $S_{[holes]}$ , expressed as curve length in mm), was measured following the surface underneath the maximum radius of the holes (Fig. 4). As the generated 3D meshes were open at their bottom (i.e. the parts which touched the seabed) these open meshes were closed automatically closed with a plan approximating the seabed, before the estimation of the hummock's volume ( $V_{[3D]}$ ).

The effective surface area of models ( $ESA_{[3D]}$ ), equivalent to the living part of a hummock, was calculated as the total surface area ( $SA_{[total]}$ ) of the colony minus the summation of the surface areas of all the holes and

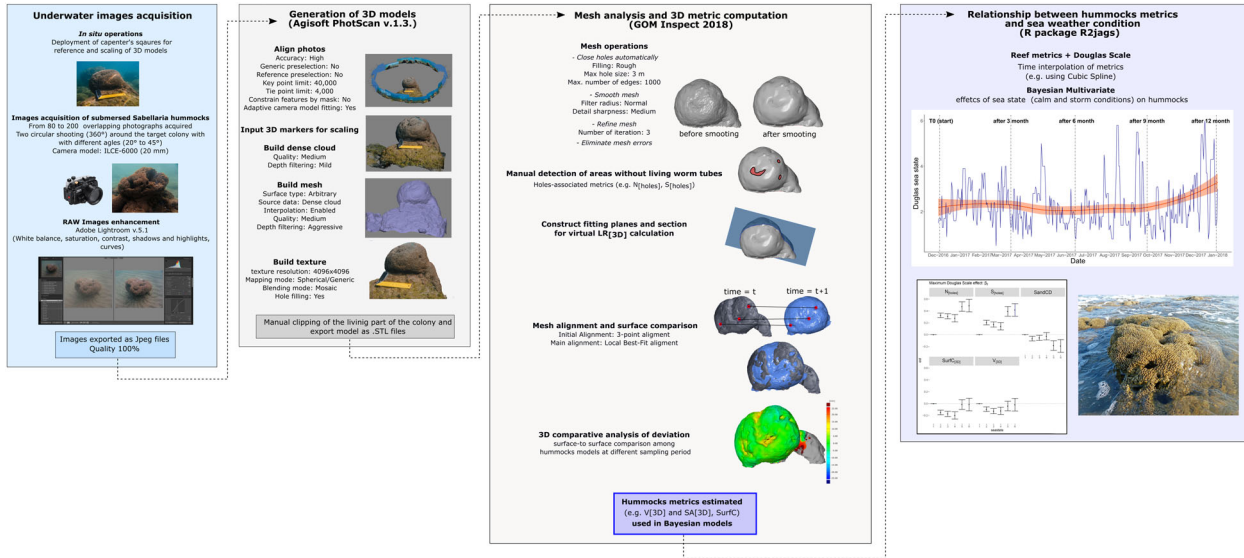


**Figure 2.** Mains steps of the workflow adopted in this work encompassing underwater digital images acquisition, photogrammetric processes (PhotoScan software), 3D model analysis (GOM Inspect software) and Bayesian multivariate analysis (R software).

crevices (i.e.  $SA_{[holes]}$ ), areas with no living worm tubes that were present on the surface of the hummock:

$$ESA_{[3D]}(m^2) = SA_{[total]}(m^2) - \sum_{i=1}^n SA_{[holes]i}(m^2) \quad (1)$$

Surface complexity (*SurfC*), a critical factor affecting ecological and physical processes on the reef, was calculated as the ratio of 3D surface area to projected planar area (i.e. surface area over the occupied planar space).

$$SurfC_{[3D]} = \frac{SA_{[3D]}}{A_{[2D]}} \quad (2)$$

In addition, we compared linear rugosity obtained from *in situ* traditional ‘chain-and-tape’ measurements ( $LR_{[chain]}$ ) and as calculated in GOM Inspect software  $LR_{[3D]}$ . To do so, we draped four virtual chains and tapes on *Sabellaria* hummocks and constructed along the Z-axis four fitting planes spaced at 45° intervals each other and perpendicular to the X-axis (i.e. the sea bottom) with the intersection point located in the center of each hummock (Fig. 5A). These four reference planes were used to generate sections on the mesh (Fig. 5B). Subsequently, the curve length (*CL*, i.e. the virtual ‘chain’) of each section was estimated and compared to the linear distance (*D*, i.e. the virtual ‘tape’) comprised between the starting and ending points of the section curve (Fig. 5C). Linear rugosity ( $LR_{[3D]}$ ) values for each surveyed colony were estimated by computing the ratio between *CL* (m) and *D* (m) across the four different fitting planes. By averaging these values, we computed a mean linear rugosity value for each surveyed colony.

$$LR_{[3D]} = \frac{\sum_{i=1}^4 \frac{CL_{[plane]i}}{D_{[plane]i}}}{4} \quad (3)$$

The number of tubes with sandy porches was estimated by overlapping four virtual 10 × 10 cm frames (Fig. S3), randomly placed on each side (N, S, W, E) of the hummock. Manual count of tubes were performed in ImageJ 1.46 (Schneider et al., 2012) by analysing different views of models’ surface, in fact by rotating 3D models we were able to better distinguish all the tube apertures facing different direction in a single frame. This step requires a priori knowledge, so only trained operator should perform the count of tubes. Subsequently, the density of living worms per colony (sand crown density or *SandCD*) was estimated by multiplying the average densities values (derived from the four virtual frames) with the effective surface area ( $ESA_{[3D]}$ ) of the colony.

$$SandCD = \left( \frac{\sum_{i=1}^4 (N_{[sand\ crown]} / m^2_{[virtual\ frames]_i})}{4} * ESA_{[3D]} \right) \quad (4)$$

The morphological change over time of each *Sabellaria* colony was assessed using 3D morphometric surface comparison (Fig. 6). To compare times *t* and *t* + 1 we set as reference the modelled surface at time *t* and aligned the analogous surface at time *t* + 1. This procedure is replicated for each pair of adjacent time points (sampling occasions). The alignment procedure involved an initial

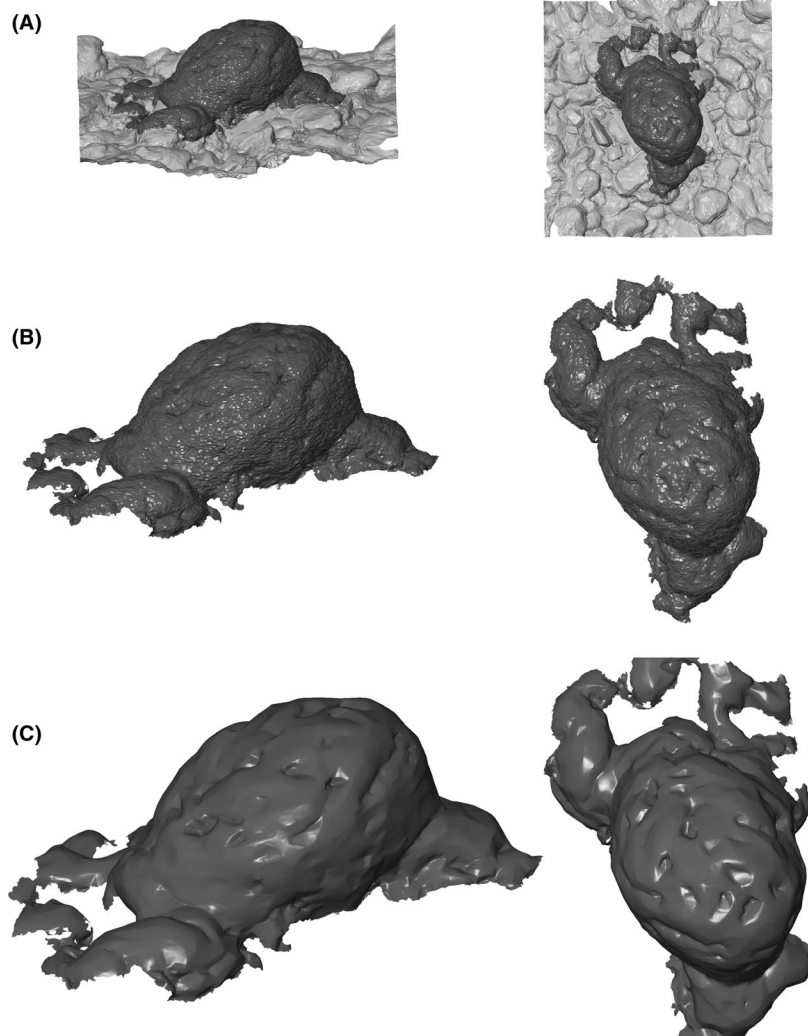


**Figure 3.** Lateral (left) and top (right) views of the 3D model generated by SfM-based underwater photogrammetry of *Sabellaria* hummock (Sab-1). (A) the living colony of individuals (in dark gray) on pebbly bottom (light gray) at 3 m depth. (B) the living part of the colony isolated from the sea bottom with an evident surface roughness generated by sandy tubes (C) Smoothed model after triangular meshes editing in GOM Inspect software.

3-point alignment, followed by a ‘best-fit’ algorithm. More precisely, the Least Squares algorithm of the Best Fit alignment aligns two sets of points by transforming one of the sets (time  $t + 1$  in our protocol) so that the sum of the squared distances between matching points in the two sets is minimal. It should be noted that this alignment procedure not implied the use of fixed reference points (independent of the accreting/eroding colony surfaces), so by minimising the differences measured on two surfaces we did not accurately represent accretion and erosion events at specific locations of the colony, however, we were able to provide a very fine scale visual overview on the processes occurring on the hummocks’ surfaces.

After this step, the software generated heat maps with differently colored areas, denoting varying degrees of deviation (in mm) between the two compared surfaces. Positive deviation from the reference model were considered as accretion (or progradation) while negative deviation denoted erosion (or retrogradation). Mean and standard deviation of morphological changes were then calculated.

#### Software measurement error

*Sabellaria* reefs along European coasts are threatened and protected by several measures, preventing the extraction of hummocks for laboratory analysis. To demonstrate the

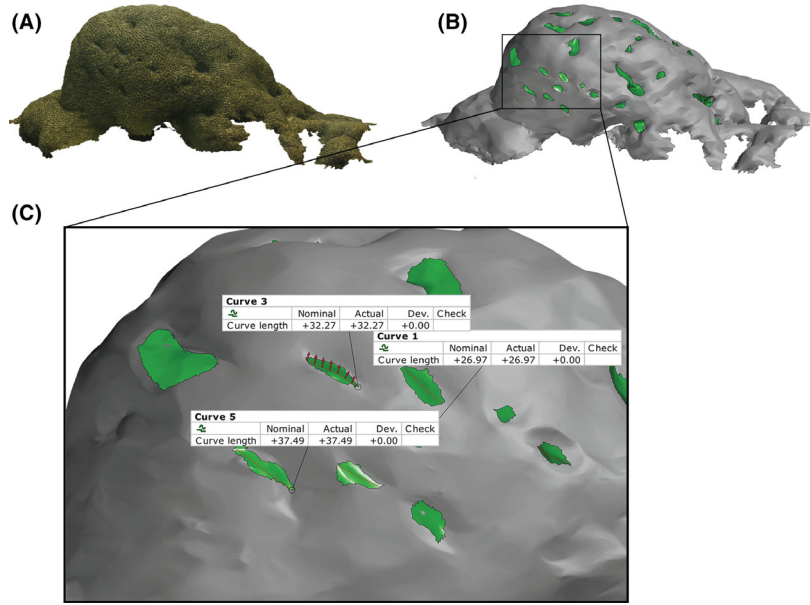


**Figure 4.** Manual detection and measurements of holes and crevices. (A) Textured 3D model from PhotoScan (B) holes highlighted in green on the 3D mesh imported as STL file in GOM Inspect software (C) a close-up view of the mesh showing non-vital areas of the colony (holes) and the estimation of their size (curve length measuring) in GOM Inspect software.

proportional accuracy and to assess procedural errors of the 3D models, we rendered pebbles and reference objects (e.g. carpenter's squares). We compared objects' known dimensions to their estimated dimensions from the models. Ten pebbles were removed from water, and their volume was determined by measuring the volume of water before and after the pebbles were held suspended in the water (i.e. water displacement method). The accuracy of a measurement for each measure (linear distance and volume) estimated from 3D models was expressed as percentage of difference (Young et al. 2017). For example, the deviation of  $V_{[3D\ estimated]}$  from  $V_{[water\ displacement]}$  was computed as follows:

$$\text{Accuracy \%} = 1 - \frac{|V_{[3D\ estimated]} - V_{[water\ displacement]}|}{V_{[water\ displacement]}} * 100 \quad (5)$$

### Statistical data analysis

For graphical visualization of *Sabellaria* metrics during the year and to better capture the global trends, the estimated metrics' values at each sampling event were interpolated by using a cubic (or Hermite) spline interpolation with equally spaced knots and the location of the knots was fixed by the sampling occasions. Spline interpolation is a robust algorithm for interpolating between sets of points which ensure that the second

derivative of the interpolated function are continuous and the first derivatives are smooth (Press et al. 2007). The same interpolation technique was used to extract the average growth rate (considered as the variation of  $V_{[3D]}$  over time which can be regarded as a good proxy for growth) between various nodes of the spline using discrete derivatives  $\left(\frac{\Delta f}{\Delta t}\right)$

### Relationship between hummocks metrics and sea weather condition

The interpolated curves were used to explore the effects of sea weather condition (according to the Douglas Scale) on *Sabellaria* hummocks. A Bayesian latent variable model approach (Press 1980) was adopted to account for correlation among variables and missing data. The interpolated values of the five metrics were first rescaled by their standard deviation and log-transformed. At this scale we assumed they can be modelled as a multivariate ANOVA-type hierarchical model. More precisely, let  $N_d$  denoted the d-dimensional Gaussian distribution hence:

$$Y|\mu, T \sim N_5(\mu, T)$$

$$\mu_{ij} = \beta_{0ij} + \beta_{1ik} + \beta_{2ih} + \beta_{3il}$$

$$\beta_{0j} \sim N_5(\mathbf{0}, \mathbf{Q}), j = 2, 3, 4,$$

$$\beta_{1k} \sim N_5(\mathbf{0}, \mathbf{Q}_1), k = 1, \dots, 6$$

$$\beta_{2h} \sim N_5(\mathbf{0}, \mathbf{Q}_1), h = 2, \dots, 6$$



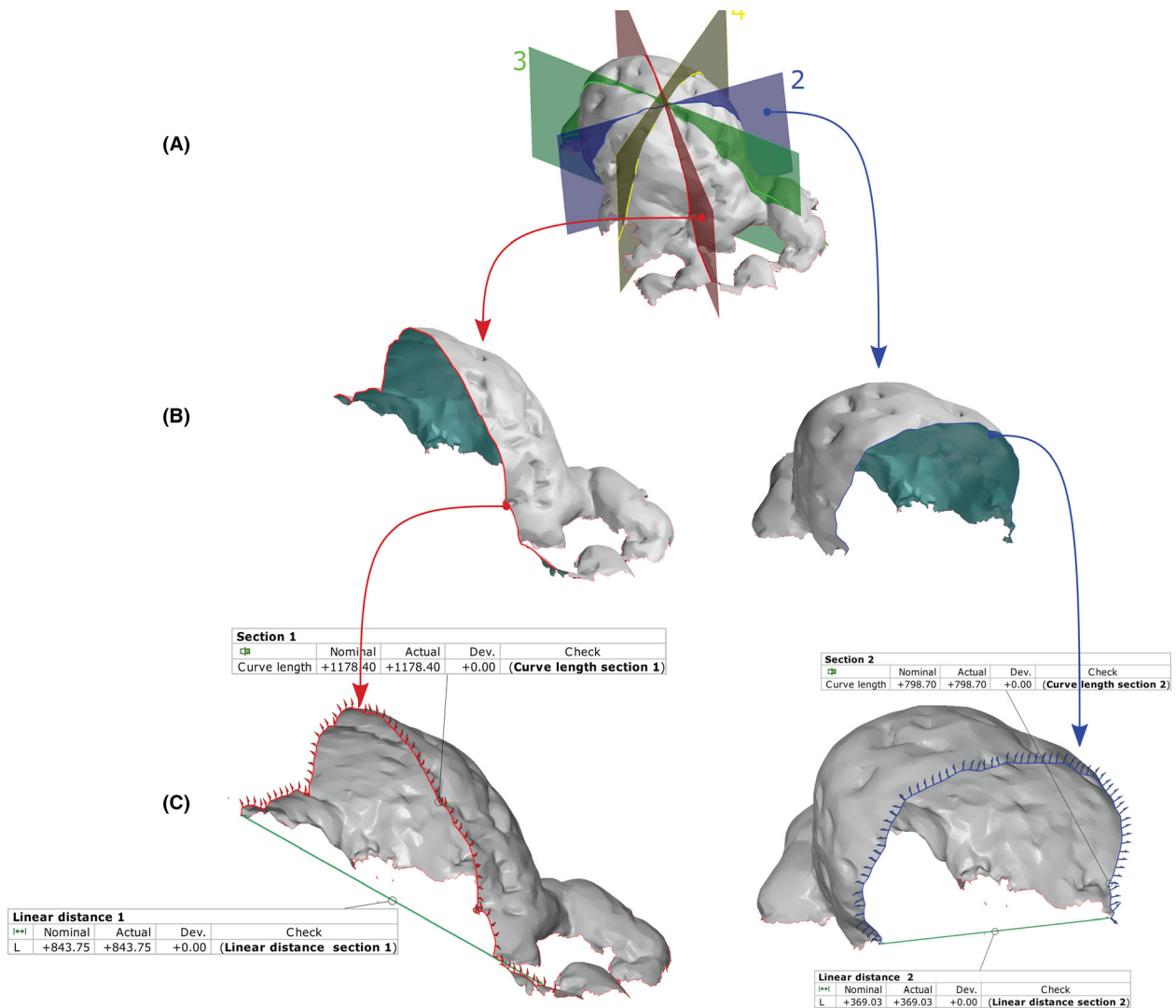


**Figure 5.** Adopted steps for quantifying linear rugosity ( $LR_{[3D]}$ ) on 3D model of a *Sabellaria* hummock using virtual ‘chain-and-tape’ method. (A) four fitting planes (1–4) perpendicular to the X-axis (i.e. the sea bottom) intersecting the center of the hummock were created in GOM Inspect software. (B) Examples of two cross sections generated according to the fitting planes 1–2. (C) Estimation of curve length (i.e. the virtual chain draped over the hummock, displayed as red and blue curves with small arrows) and linear distance (D, i.e. the virtual tape measure, displayed as green line) used for linear rugosity estimation.

$$\beta_{3l} \sim N_5(\mathbf{0}, \mathbf{Q}_1), l = 1, 2$$

$$\tau_j^2 \sim \text{Gamma}(2, 2), j = 1, 2, 3, 4$$

$$\mathbf{Q} \sim \text{Wishart}(\mathbf{R}, 15)$$

where  $t = 1, \dots, 1588$  was the observation index,  $i = 1, \dots, 5$  denoted the metric ( $V_{[3D]}$ ,  $SurfC_{[3D]}$ ,  $N_{[holes]}$ ,  $S_{[holes]}$  and  $SandCD$ ),  $j = 1, 2, 3, 4$  was the hummock label,  $k = 0, \dots, 6$  was the minimum of the Douglas Scale recorded in the day,  $h = 1, \dots, 6$  is the maximum of the Douglas Scale recorded in the day and  $l = 1, 2, 3,$

distinguish between three quarters defined as late autumn – winter (November, December, January and February), spring-early summer (March, April, May, June) and late summer – early autumn (July, August, September, October).  $T$  was a block diagonal precision matrix with diagonal elements  $\tau_j^2$  denoting the residual precision associated to each colony.  $\mathbf{Q}$  was the precision matrix accounting for the correlation among the metrics and its distributed as a Wishart distribution with parameters given by the empirical correlation among the metrics and 15 degrees of freedom that allowed for a large variability of all matrix elements, eventually  $\mathbf{Q}_t$  was obtained by rescaling

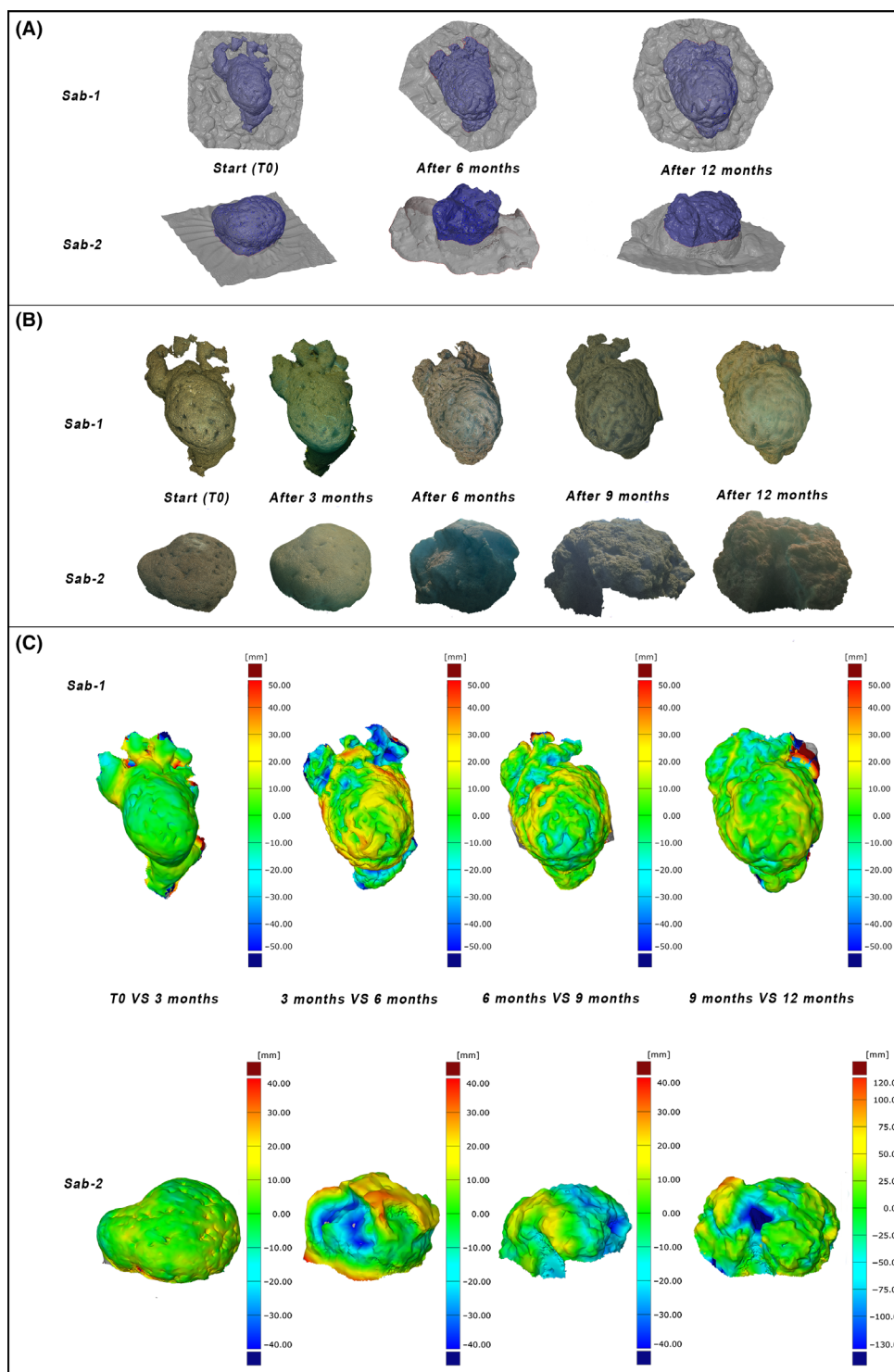


**Figure 6.** Example of morphological changes over time in two *Sabellaria* hummocks (Sab-1 and Sab-2) achieved in GOM Inspect software. (A) 3D models of *Sabellaria* hummocks at different sampling times: the living part (highlighted in blue) was isolated from the background. (B) Top (Sab-1) and lateral (Sab-2) views of 3D textured models showing the temporal evolution of the two hummocks. (C) Visualization of surface comparison between 3D models. Colored areas represent varying degrees of deviation (in mm) between the two compared surfaces. Yellow-reddish areas (denoting accretion) of the model are positioned above the surface of the reference model, while the blue areas (denoting erosion) are positioned below.

$Q$  of 0.01 to ensure smaller precisions for the joint distributions of  $\beta_1, \beta_2, \beta_3$ . A corner point choice was made setting the hummock labelled Sab-1, the minimum Douglas scale value 0, the maximum Douglas Scale value 1 and the late summer – early autumn categories to zero.

$$\beta_{01} = \beta_{10} = \beta_{21} = \beta_{33} = 0$$

The model has been chosen among many others on the basis of the Deviance Information Criterion (DIC) (Spiegelhalter et al. 2014). Estimation was carried out using the software JAGS (Plummer 2003) and the R package R2jags (Su and Yajima, 2015). The specific code is available as supplementary material.

## Results

### Accuracy of 3D models

Dimensions on the underwater 3D models of pebbles used for calibration purposes matched strongly with their true dimensions: procedural accuracy for length and volume were 97.73% ( $SD = \pm 0.002$ ) and 97.9% ( $SD = \pm 0.001$ ), respectively. Significant linear correlations were found between the real dimensions of the pebbles and their estimated values from models ( $R^2 > 0.99$ ,  $P < 0.001$ , both for length and volume, Fig. S4). The slopes  $< 1$  (0.98 and 0.93 for length and volume, respectively) of the regression plots indicate that both length and volume estimated from 3D models slightly overestimated the real dimensions of the objects.

### 3D model-based metrics and temporal change detection

Both  $SurfC_{[3D]}$  and  $LR_{[3D]}$  estimated from 3D models are strongly correlated ( $R^2 = 0.82$ ,  $t = 76.09$ ,  $P < 0.005$  for  $SurfC_{[3D]}$  and  $R^2 = 0.86$ ,  $t = 103.5$ ,  $P < 0.001$  for  $LR_{[3D]}$ ) with *in situ* chain-and-tape measurements (Fig. S5). The metric  $LR_{[3D]}$  showed a clear correlation ( $R^2 = 0.88$ ,  $t = 120.3$ ,  $P < 0.001$ ) with  $SurfC_{[3D]}$ , confirming that both methods well depicted the morphological complexity of hummocks' surfaces.

$V_{[3D]}$  and  $SA_{[3D]}$  values (Fig. 7A and B) are both measurements of the accretion/erosion of *Sabellaria* colonies and were strongly correlated (Pearson's correlation = 0.97,  $t = 18.919$ , d.f. = 16,  $P$ -value =  $< 0.001$ ). They showed an increasing trend with maximum values recorded after 6 months (mid-June) for the three isolated *Sabellaria* hummocks (Sab-1, Sab-2 and Sab-3). After this timespan a decline of both metrics was reported for the first two large isolated hummocks ( $V_{[3D]} = 0.043 \text{ m}^3$  and  $V_{[3D]} = 0.1 \text{ m}^3$  for Sab-1 and Sab-2, respectively) and the smallest hummock (Sab-3,  $V_{[3D]} = 0.0086$ ) was

completely disintegrated by waves. The peak of growth of Sab-4 was recorded after 9 months and after this period both  $V_{[3D]}$  and  $SA_{[3D]}$  followed a strong decline like the other two hummocks. The lowest values of  $SurfC_{[3D]}$  (Fig. 7C) were reported after 3 months (mid-March) for the first three hummocks ( $SurfC_{[3D]} = 1.83, 2.19$  and  $3.43$  for Sab-1 to Sab-3, respectively) and after this period the surface complexity increased with highest values reported in winter during the last sampling carried out at the end of December 2017. The smallest hummock (Sab-3) showed the highest values of  $SurfC_{[3D]}$  compared to other hummocks. A small number ( $N_{[holes]}$ ) and size ( $S_{[holes]}$ ) of holes (Fig. 7D and E) were reported when the colonies were in expansion (first six months for the first three hummocks and up to the ninth months for the fourth hummock), subsequently  $N_{[holes]}$  increased after the summer period, whereas  $S_{[holes]}$  after reaching the peak (after 6 or 9 months, depending on the hummock) tended to decrease. It is worth noticing that other general relationships detected for each hummock (i.e. erosion vs accretion) also exhibited fine scale variability linked to the presence of surface irregularities such as holes. This variability is key in explaining local erosion processes affecting colonies' surfaces, as well as major erosion events adversely affecting damaged or weakened bioconstructions (e.g. Sab-2 in Fig. 6).  $SandCD$  (Fig. 7F) was inversely correlated (Pearson's correlation = 0.86,  $t = -6.8931$ , d.f. = 16,  $P$ -value  $< 0.001$ ) with  $SurfC_{[3D]}$  and the highest values were reported after 3 months (Avg.  $SandCD_{[1-3 \text{ months}]} = 9691$ ,  $SD = 41$ ;  $10327$ ,  $SD = 2275$ ;  $5002$ ,  $SD = 536$  for Sab-1 to Sab-3, respectively) and six months for Sab-4 (Avg.  $SandCD_{[1-3 \text{ months}]} = 9395.35$ ,  $SD = 1127$ ) then  $SandCD$  tended to decrease, reaching the lowest values at the end of the year.

### Reef growth and effects of storms

Considering all the sampled colonies we reported a volumetric change of the reef (Fig. S6) with a mean monthly increment of 12.92 % ( $SE = \pm 0.07\%$ ) in the first nine months (from December 2016 until the end of September 2017). Subsequently, an erosion with a net loss of bioconstruction of  $-29.53\%$  ( $SD = 0.3\%$ ) was observed during winter 2017.

During deviations inspection, positive deviations (i.e. accretion) were reported for the first six months (from December 2016 until mid-June 2017) for Sab-1, Sab-2 and Sab-3. The smallest colony (Sab-3) showed largest positive deviation indicating a quick development of the colony compared to the others. After the growth period surface-to-surface comparison showed large negative deviations (i.e. erosion) for all hummocks during the winter season (from ninth month to the end of the year). The

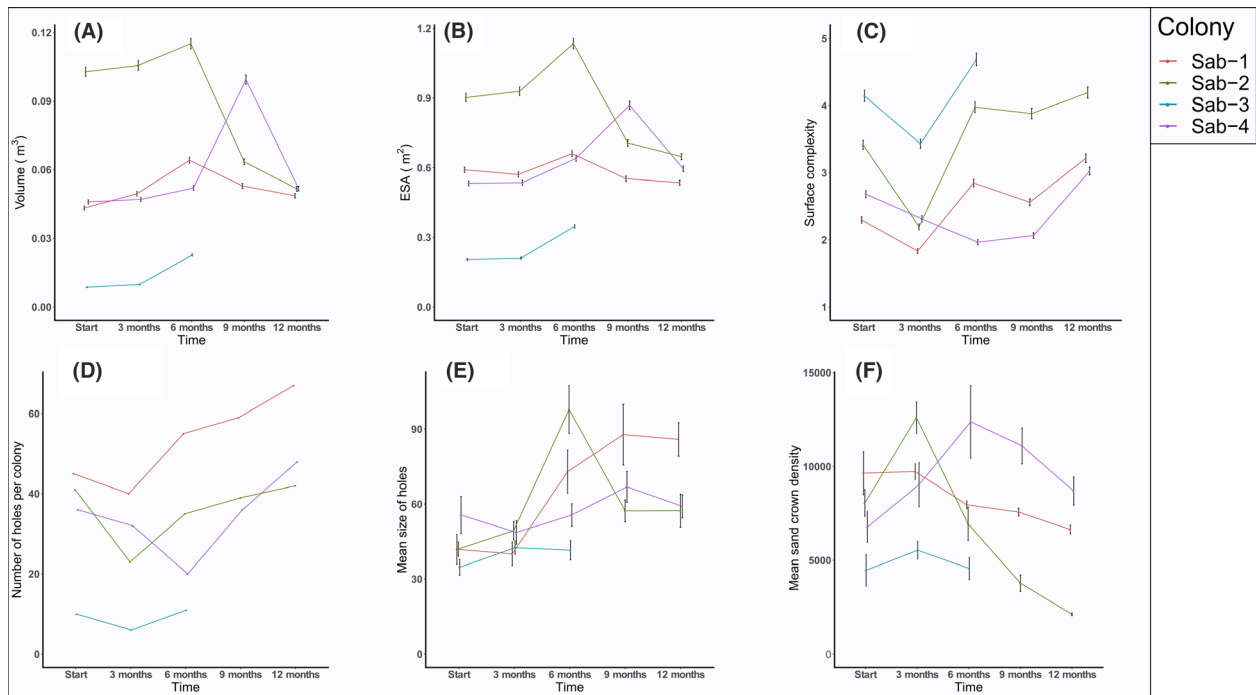


**Figure 7.** Interpolated values showing the temporal change among the five samplings (x-axis) of 3D model-based metrics (y-axis) for the four *S. alveolata* hummocks. (A)  $V_{[3D]}$ . (B)  $ESA_{[3D]}$ . (C)  $SurfC_{[3D]}$ . (D)  $N_{[holes]}$ . (E)  $S_{[holes]}$ . (F)  $SandCD$ . Error bars in A, B and C represent  $\pm 3\%$  measurement error and  $\pm SE$  in E and F.

fourth hummock (Sab-4) showed a similar trend for the first six months but its growth continued until the ninth month followed by a large decline at the end of the year (Fig. 8).

Bayesian latent variable model provided a good fit for all the *Sabellaria* metrics ( $V_{[3D]}$ ,  $SurfC_{[3D]}$ ,  $N_{[holes]}$ ,  $S_{[holes]}$  and  $SandCD$ , Fig. S7) against Douglas scale values with very low residual variance explained for the four hummocks (Fig. S8). The model showed significant effects for the sea state at hummock level for all the considered metrics (Fig. 9A), with the smallest hummock (Sab-3) clearly separated from the others. In particular, the high values of the Douglas's scale showed a significant effects both on the number and size of holes ( $N_{[holes]}$  and  $S_{[holes]}$ ) and on the density of sand crown ( $SandCD$ ) (Fig. 9B) while minimum values did not show significant effects on none of the considered metrics (Fig. 9C).  $SurfC_{[3D]}$  and  $V_{[3D]}$  did not show a specific relation with largest values of the maximum Douglas scale, but they interacted with the sea state in a more homogeneous way probably because of growth effects took place constantly even during bad weather periods. They showed a significant seasonal effect due to storm events at the end of the summer (late summer- early autumn) and during the winter (late autumn-winter) seasons (Fig. 9D).  $SurfC_{[3D]}$  is affected in the same way by events in spring-early summer and in late

autumn-winter while  $V_{[3D]}$  is clearly strongly reduced by events during the colder season.

## Discussion

In this study, we demonstrated that a relatively low-cost SfM close-range photogrammetry approach (the whole equipment used was under 4000\$) could be a non-invasive method to accurately measure volume and surface area of underwater Sabellariid bioconstructions. SfM process renders textured 3D models in multiple file formats that serve as powerful visualization tools for assessing the dynamics of structural complexity in biogenic reef environments. Moreover, 3D models can also be used to follow growth rates as well as morphology changes over time providing high accuracy assessments on the dynamics (erosion and growth) of *S. alveolata* reefs. Overall, the results indicate that measurements taken from 3D modelled hummocks that compose a reef habitat can be treated with a high degree of confidence showing an average measurement error = 3% ( $SD = 0.23\%$ ) considering both volume and linear distances. Our accuracy tests were carried out on pebbles and small boulders which could be removed and carried to the laboratory for volumetric estimates by water displacement, so the tested range was limited to 50.6–1667  $cm^3$  while the largest *Sabellaria* colony



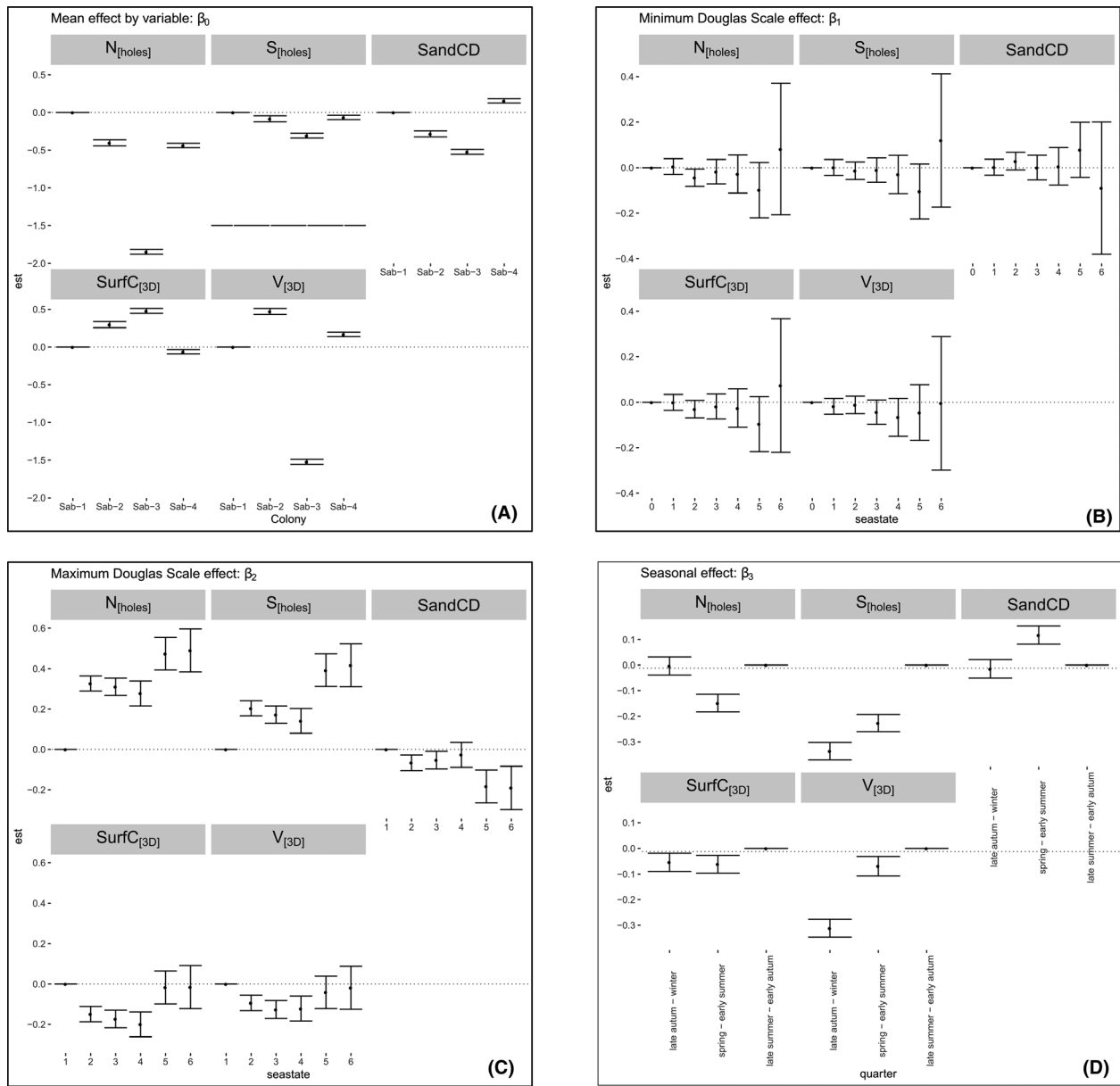


**Figure 9.** Plots representing the estimated effects of sea state (Douglas scale) on the main *Sabellaria* metrics ( $N_{[holes]}$ ,  $S_{[holes]}$ ,  $SurfC_{[3D]}$ ,  $SandCD$  and  $V_{[3D]}$ ) estimated from 3D model analysis. (A) Mean effects per variable –  $\beta_0$ . (B) Minimum Douglas scale effects –  $\beta_1$ . (C) Maximum Douglas scale effects –  $\beta_2$ . (D) Seasonal effects –  $\beta_3$ . Note that significant effects are highlighted by segments (representing 95% confidence intervals around specific effects size) not crossing the zero line.

occurring in the volumetric and structural properties of the colony. This will be critical for accurately investigating environmental effects influencing reef biomass and structure at very small scale. In fact, reef rugosity modifies wave processes and bedload sediment transportation and is key ecological indicator as the physical structures, providing complex benthic habitats which have been shown to strongly correlate with fish diversity and coral community composition (Leon et al. 2015). Moreover it is also

essential for determining how colonies will respond to external stressors, such as strong storms and anthropogenic impacts, because quantifying accretion and erosion rates could play a pivotal role to understand the bioconstruction’s resistance to perturbations (i.e. how much the reef habitat changes) and its resilience (i.e. to what extent the reef can recover after the source of perturbation is removed). Ultimately, providing quantitative metrics will drastically help management plans of coastal

areas where bioconstructions are developing. To date, there are significant information gaps to assess recovery rates, stability or persistence in *Sabellaria* reefs. Studies suggested that surficial damage within reefs may be rapidly repaired by the tube building activities of adult worms. For instance trawl impressions made in *S. spinulosa* reefs disappeared five days later due to the rapid rebuilding of tubes (Vorberg 2000). However, severe damage caused heavy trampling on the reef structure, resulted in large cracks between the tubes with other cumulative negative effects of wave action on these holes (Gibb et al. 2014; Plicanti et al. 2016). Since hydrodynamics could be considered the main physical factor influencing the succession of colonies (Gruet 1986), we analysed the effects of sea state (expressed as mean daily values of Douglas scale) on *Sabellaria* hummocks. Despite the strengthen of biogenic sand reefs due to bio-mineralized cement which behaves like a visco-elastic material allowing the tubes to dissipate the mechanical energy from the waves (Le Cam et al. 2011) we highlighted that major storms could impact *Sabellaria* colonies during their mushroom-like stages. During very high hydrodynamic conditions also *SandCD* was reduced confirming that erosion also affected the tubes densities which can be regarded as a good proxy for the health status of the reef and populations structure. We reported that high waves destroyed Sab-3 which disappeared after five months. Intense wave energy can alter reef structure through two main processes: either directly by disrupting entire hummocks and collapsing large reef areas or indirectly by setting into motion shell fragments, gravels or pebbles that in turn damage tube openings and erode holes and cervices where the bioconstruction is already more fragile. This mechanical perturbation is well evidenced by the survey provided in this study (see Fig. 6 for example). Moderate sea state condition conversely (waves from 0.10 to 2.5 m, up to fourth grade according the Douglas scale) seemed to favor the growth phase of the colonies (as confirmed by the increase of  $V_{[3D]}$  and  $SA_{[3D]}$  values during the first six months). Under moderate hydrodynamic condition, only sand particles and small shell fragment are resuspended, which ultimately stimulate tube-building activity. In that case, wave agitation had positive role in reef enlargement as it ensured both food and sand particles to worms (Gruet 1986). However, further studies should be carried out to better define the role of hydrodynamic conditions on biogenic *Sabellaria* reefs, especially if detailed and quantitative data on sea state and hydrodynamic conditions could be implemented in the analysis.

During the growth phase of colonies,  $SurfC_{[3D]}$  showed a clear drop which indicated that when the bio-constructions were in good condition (also confirmed by the high *SandCD* values for these periods) the individuals tended

to fill in cracks and holes between tubes making the surface morphology more compact and continuous. The approach tested here show that we can monitor and map recruitment patterns at a fine scale. Recruitment of juveniles is a key element for a reef structure to maintain and resist against various damaging pressures, as newly arrivals on a reef start immediately building new tubes and enhance the tube-building activity of surrounding adults. However, we mapped growth patterns and recruitment on a very local scale using an indirect method (i.e. the number of sand crowns considered as a proxy for living worms), but recruitment patterns occurring in the four monitored colonies did not constitute mapping of patterns at the reef scale. For this reason, further works based on this method will be carried out to scale up to habitat scale monitoring in order to represent the whole reef with the same spatial resolution allowing the estimation of other complex seascape metrics implemented in specific software often used in ecology such as FRAG-STATS (McGarigal et al. 1995). Obviously, to expand the sampling area covered, preserving the same spatial resolution, semi-autonomous underwater vehicles could become an important tool to support SfM-based imagery as already demonstrated in tropical environments (Palma et al. 2017).

## Conclusions

Long-term changes of sabellariid reefs were finely described at Champeaux (Mont-Saint-Michel Bay, NW France) and at Duckpool in north Cornwall (Wilson 1971; Gruet 1986). These studies used transects and reef pictures to show cyclic changes in reef phases, but they were not able to map changes and link them with environmental effects. In fact, characterizing and monitoring change in biogenic 3-dimensional structures at multiple scales over time is challenging within the practical constraints of conventional ecological tool (D'Urban Jackson et al. 2020). However, our work highlights how new advances in computer vision and processing techniques of close-range photogrammetry-based imagery can be used for fine scale analysis of ecological metrics of similar *S. alveolata* reefs. We demonstrated that strong changes of reef morphology could occur also at very small scale (hummock level) during a limited time span (1 year) due to water agitation which played firstly a positive role then a negative effect, leading to the destruction of hummocks when strong hydrodynamics forces took place during severe storm events. Therefore, sabellariid bioconstruction morphology is the result of a complex set of biological and physical factors shaping the reef. We reported that erosion rates (loss of colonies' volume) occurred faster than growth rates. These findings could open new lines of

research aimed at minimizing the impact on intertidal reefs, especially if we consider that the Mediterranean *scenario* for the next years will be characterized by an increase in the intensity and frequency of sea surges because of climate change (Marcos et al. 2011).

It is our hope that this study will provide a methodological platform for future studies to accurately quantify 3D properties of sabellariid reefs. In fact, sub-mm resolution underwater photogrammetry coupled with powerful inspection and mesh processing software could improve both our collective understanding of these important ecosystems and serve as a proof of concept aimed at implementing this relatively fast, flexible, low-cost and non-intrusive sampling methods for short and long-term monitoring of benthic organisms, such as temperate biogenic bioconstructions.

## Acknowledgments

This study was supported by small research projects funding program of the Department of Environmental Biology and Ecology, University of Rome 'La Sapienza'. D.V. thanks Veronica for her love and support during field operations and sampling activities. The authors thank their colleagues Dr. G. Mancini, Dr. E. Casoli and Dr. A. Belluscio for their valuable support and suggestions. All the authors extend their appreciation toward the three anonymous Reviewers for taking the time and effort necessary to provide such insightful guidance.

## Authors' contributions

D.V. conceived and designed the study in collaboration with S.D., A.B., M.F. G.A. and M.S. obtained funding for the fieldwork and equipment. D.V. conducted the fieldwork with logistic support from G.A., D.V., G.J.L. and S.D., analysed the data and wrote the manuscript. All authors contributed to subsequent drafts and gave final approval for publication and declare no conflict of interest.

## References

Ayata, S.-D., C. Ellien, F. Dumas, S. Dubois, and É. Thiébaud. 2009. Modelling larval dispersal and settlement of the reef-building polychaete *Sabellaria alveolata*: role of hydroclimatic processes on the sustainability of biogenic reefs. *Cont. Shelf Res.* **29**, 1605–1623.

Bamber, R. N., and P. W. Irving. 1997. The differential growth of *Sabellaria alveolata* (L.) reefs at a power station outfall. *Polychaete Res.* **17**, 1–12.

Bonifazi, A., M. Lezzi, D. Ventura, S. Lisco, F. Cardone, and M. F. Gravina. 2019. Macrofaunal biodiversity associated with different developmental phases of a threatened

Mediterranean *Sabellaria alveolata* (Linnaeus, 1767) reef. *Mar. Environ. Res.* **145**, 97–111. <https://doi.org/10.1016/j.marenvres.2019.02.009>

Bruschetti, M. 2019. Role of reef-building, ecosystem engineering polychaetes in shallow water ecosystems. *Diversity* **11**, 168.

Burns, J. H. R. R., D. Delparte, R. D. Gates, and M. Takabayashi. 2015. Integrating structure-from-motion photogrammetry with geospatial software as a novel technique for quantifying 3D ecological characteristics of coral reefs. *PeerJ* **3**, e1077.

Cocito, S., S. Sgorbini, A. Peirano, and M. Valle. 2003. 3-D reconstruction of biological objects using underwater video technique and image processing. *J. Exp. Mar. Biol. Ecol.* **297**, 57–70.

Collin, A., S. Dubois, C. Ramambason, and S. Etienne. 2018. Very high-resolution mapping of emerging biogenic reefs using airborne optical imagery and neural network: the honeycomb worm (*Sabellaria alveolata*) case study. *Int. J. Remote Sens.* **39**, 5660–5675.

Collin, A., S. Dubois, D. James, and T. Houet. 2019. Improving intertidal reef mapping using UAV surface, red edge, and near-infrared data. *Drones* **3**, 67.

Curd, A., F. Pernet, C. Corporeau, L. Delisle, L. B. Firth, F. L. D. Nunes, et al. 2019. Connecting organic to mineral: how the physiological state of an ecosystem-engineer is linked to its habitat structure. *Ecol. Ind.* **98**, 49–60.

D'Urban Jackson, T., G. J. Williams, G. Walker-Springett, and A. J. Davies. 2020. Three-dimensional digital mapping of ecosystems: a new era in spatial ecology. *Proc. R. Soc. B* **287**, 20192383.

Desroy, N., S. F. Dubois, J. Fournier, L. Ricquiers, P. Le Mao, L. Guerin, et al. 2011. The conservation status of *Sabellaria alveolata* (L.) (Polychaeta: Sabellariidae) reefs in the Bay of Mont-Saint-Michel. *Aquat. Conserv.* **21**, 462–471.

Dubois, S., C. Retière, and F. Olivier. 2002. Biodiversity associated with *Sabellaria alveolata* (Polychaeta: Sabellariidae) reefs: effects of human disturbances. *J. Mar. Biol. Assoc. U.K.* **82**, 817–826.

Dubois, S., J. A. Commito, F. Olivier, and C. Retière. 2006. Effects of epibionts on *Sabellaria alveolata* (L.) biogenic reefs and their associated fauna in the Bay of Mont Saint-Michel. *Estuar. Coast. Shelf Sci.* **68**, 635–646.

Dubois, S., T. Comtet, C. Retière, and E. Thiébaud. 2007. Distribution and retention of *Sabellaria alveolata* larvae (Polychaeta: Sabellariidae) in the Bay of Mont-Saint-Michel, France. *Mar. Ecol. Prog. Ser.* **346**, 243–254.

Dubois, S., L. Barillé, and B. Cognie. 2009. Feeding response of the polychaete *Sabellaria alveolata* (Sabellariidae) to changes in seston concentration. *J. Exp. Mar. Biol. Ecol.* **376**, 94–101.

Ferrari, R., W. F. Figueira, M. S. Pratchett, T. Boube, A. Adam, T. Kobelkowsky-Vidrio, et al. 2017. 3D



- photogrammetry quantifies growth and external erosion of individual coral colonies and skeletons. *Sci. Rep.* **7**, 16737.
- Figueira, W., R. Ferrari, E. Weatherby, A. Porter, S. Hawes, and M. Byrne. 2015. Accuracy and precision of habitat structural complexity metrics derived from underwater photogrammetry. *Remote Sens.* **7**, 16883–16900.
- Friedman, A., O. Pizarro, S. B. Williams, and M. Johnson-Roberson. 2012. Multi-scale measures of rugosity, slope and aspect from benthic stereo image reconstructions. *PLoS One* **7**, e50440.
- Fukunaga, A., J. H. R. Burns, B. K. Craig, and R. K. Kosaki. 2019. Integrating three-dimensional benthic habitat characterization techniques into ecological monitoring of coral reefs. *J. Mar. Sci. Eng.* **7**, 27.
- Gibb, N., H. M. Tillin, B. Pearce, and H. Tyler-Walters. 2014. Assessing the sensitivity of *Sabellaria spinulosa* to pressures associated with marine activities.
- Goldberg, W. M. 2013. *The biology of reefs and reef organisms*. Chicago IL: University of Chicago Press.
- Gravina, M. F., F. Cardone, A. Bonifazi, M. S. Bertrandino, G. Chimienti, C. Longo, et al. 2018. *Sabellaria spinulosa* (Polychaeta, Annelida) reefs in the Mediterranean Sea: habitat mapping, dynamics and associated fauna for conservation management. *Estuar. Coast. Shelf Sci.* **200**, 248–257.
- Gruet, Y. 1986. Spatio-temporal changes of sabellarian reefs built by the sedentary polychaete *Sabellaria alveolata* (Linné). *Mar. Ecol.* **7**, 303–319.
- Gutierrez-Heredia, L., F. Benzoni, E. Murphy, and E. G. Reynaud. 2016. End to end digitisation and analysis of three-dimensional coral models, from communities to corallites. *PLoS One* **11**, e0149641.
- Harborne, A. R., P. J. Mumby, and R. Ferrari. 2012. The effectiveness of different meso-scale rugosity metrics for predicting intra-habitat variation in coral-reef fish assemblages. *Environ. Biol. Fishes* **94**, 431–442.
- Harrison, R., F. Bianconi, R. Harvey, and W. Wang. 2011. A texture analysis approach to identifying sabellaria spinulosa colonies in sidescan sonar imagery. Pp. 58–63 in *Proceedings - 2011 Irish Machine Vision and Image Processing Conference, IMVIP 2011*. Dublin: IEEE.
- House, J. E., V. Brambilla, L. M. Bidaut, A. P. Christie, O. Pizarro, J. S. Madin, and et al. 2018. Moving to 3D: relationships between coral planar area, surface area and volume. *PeerJ* **6**, e4280.
- Jones, A. G., S. F. Dubois, N. Desroy, and J. Fournier. 2018. Interplay between abiotic factors and species assemblages mediated by the ecosystem engineer *Sabellaria alveolata* (Annelida: Polychaeta). *Estuar. Coast. Shelf Sci.* **200**, 1–18.
- Lavy, A., G. Eyal, B. Neal, R. Keren, Y. Loya, and M. Ilan. 2015. A quick, easy and non-intrusive method for underwater volume and surface area evaluation of benthic organisms by 3D computer modelling. *Methods Ecol. Evol.* **6**, 521–531.
- Lawton, J. H., and C. G. Jones. 1995. Linking species and ecosystems: organisms as ecosystem engineers. Pp. 141–150 in C.G. Jones and J.H. Lawton, eds. *Linking species & ecosystems*. New York: Springer.
- Le Cam, J. B., J. Fournier, S. Etienne, and J. Couden. 2011. The strength of biogenic sand reefs: visco-elastic behaviour of cement secreted by the tube building polychaete *Sabellaria alveolata*, Linnaeus, 1767. *Estuar. Coast. Shelf Sci.* **91**, 333–339. <https://doi.org/10.1016/j.ecss.2010.10.036>
- Leon, J. X., C. M. Roelfsema, M. I. Saunders, and S. R. Phinn. 2015. Measuring coral reef terrain roughness using ‘Structure-from-Motion’ close-range photogrammetry. *Geomorphology* **242**, 21–28.
- Marcos, M., G. Jordà, D. Gomis, and B. Pérez. 2011. Changes in storm surges in southern Europe from a regional model under climate change scenarios. *Global Planet. Change* **77**, 116–128.
- McCormick, M. I. 1994. Comparison of field methods for measuring surface topography and their associations with a tropical reef fish assemblage. *Mar. Ecol. Prog. Ser.* **112**, 87–96.
- McGarigal, K., and B. J. Marks. 1995. FRAGSTAT quantifying landscape structure. General Techn ment of Agriculture, Forest Service, Pacific Nort
- Naumann, M. S., W. Niggel, C. Laforsch, C. Glaser, and C. Wild. 2009. Coral surface area quantification—evaluation of established techniques by comparison with computer tomography. *Coral Reefs* **28**, 109–117. <https://doi.org/10.1007/s00338-008-0459-3>
- Naylor, L. A., and H. A. Viles. 2000. A temperate reef builder: an evaluation of the growth, morphology and composition of *Sabellaria alveolata* (L.) colonies on carbonate platforms in South Wales. *Geol. Soc. Spec. Pub.* **178**, 9–19. Available at: <http://sp.lyellcollection.org/lookup/doi/10.1144/GSL.SP.2000.178.01.02>
- Noernberg, M. A., J. Fournier, S. Dubois, and J. Populus. 2010. Using airborne laser altimetry to estimate *Sabellaria alveolata* (Polychaeta: Sabellariidae) reefs volume in tidal flat environments. *Estuar. Coast. Shelf Sci.* **90**, 93–102. <https://doi.org/10.1016/j.ecss.2010.07.014>
- Palma, M., M. Rivas Casado, U. Pantaleo, and C. Cerrano. 2017. High resolution orthomosaics of African coral reefs: a tool for wide-scale benthic monitoring. *Remote Sens.* **9**, 705.
- Pittman, S. J., and K. A. Brown. 2011. Multi-scale approach for predicting fish species distributions across coral reef seascapes. *PLoS One* **6**, e20583.
- Plicanti, A., R. Domínguez, S. F. Dubois, and I. Bertocci. 2016. Human impacts on biogenic habitats: effects of experimental trampling on *Sabellaria alveolata* (Linnaeus, 1767) reefs. *J. Exp. Mar. Biol. Ecol.* **478**, 34–44. <https://doi.org/10.1016/j.jembe.2016.02.001>
- Plummer, M. 2003. JAGS: a program for analysis of Bayesian graphical models using Gibbs sampling. P. 10 in K. Hornik, F. Leisch and A. Zeileis, eds. *Proceedings of the 3rd*

- international workshop on distributed statistical computing. Vienna, Austria.
- la Porta, B., and L. Nicoletti. 2009. *Sabellaria alveolata* (Linnaeus) reefs in the central Tyrrhenian Sea (Italy) and associated polychaete fauna. *Zoosymposia* **2**, 527–536.
- Press, S. J. 1980. 4 Bayesian inference in MANOVA. *Handbook of Statistics* **1**, 117–132.
- Press, W. H., S. A. Teukolsky, W. T. Vetterling, and B. P. Flannery. 2007. *Numerical recipes 3rd edition: the art of scientific computing*. New York: Cambridge University Press.
- Raoult, V., P. A. David, S. F. Dupont, C. P. Mathewson, S. J. O'Neill, N. N. Powell, et al. 2016. GoPro<sup>TM</sup> as an underwater photogrammetry tool for citizen science. *PeerJ* **4**, e1960.
- Raoult, V., S. Reid-Anderson, A. Ferri, and J. Williamson. 2017. How reliable is structure from motion (SfM) over time and between observers? A case study using coral reef bommies. *Remote Sens.* **9**, 740.
- Rossi, P., C. Castagnetti, A. Capra, A. J. Brooks, and F. Mancini. 2019. Detecting change in coral reef 3D structure using underwater photogrammetry: critical issues and performance metrics. *Appl. Geomat.* **12**, 1–15.
- Schneider, C. A., W. S. Rasband, and K. W. Eliceiri. 2012. NIH Image to ImageJ: 25 years of image analysis. *Nat. Methods* **9**, 671.
- Spiegelhalter, D. J., N. G. Best, B. P. Carlin, and A. Van Der Linde. 2014. The deviance information criterion: 12 years on. *J. Roy. Stat. Soc. Ser B* **76**, 485–493.
- Storlazzi, C. D., P. Dartnell, G. A. Hatcher, and A. E. Gibbs. 2016. End of the chain? Rugosity and fine-scale bathymetry from existing underwater digital imagery using structure-from-motion (SfM) technology. *Coral Reefs* **35**, 889–894.
- Su, Y.-S., and M. Yajima. 2015. R2jags: Using R to run 'JAGS'. R package version 0.5-7 34.
- Ventura, D., A. Bonifazi, M. F. Gravina, A. Belluscio, and G. Ardizzone. 2018. Mapping and classification of ecologically sensitive marine habitats using unmanned aerial vehicle (UAV) imagery and Object-Based Image Analysis (OBIA). *Remote Sens.* **10**, 1331.
- Verhoeven, G. 2011. Taking computer vision aloft—archaeological three-dimensional reconstructions from aerial photographs with photostan. *Archaeol. Prospect.* **18**, 67–73.
- Vorberg, R. 2000. Effects of shrimp fisheries on reefs of *Sabellaria spinulosa* (Polychaeta). *ICES J. Mar. Sci.* **57**, 1416–1420.
- Wilson, D. P. 1971. Sabellaria colonies at Duckpool, North Cornwall, 1961–1970. *J. Mar. Biol. Assoc. U.K.* **51**, 509–580.
- Young, G. C., S. Dey, A. D. Rogers, and D. Exton. 2017. Cost and time-effective method for multi-scale measures of rugosity, fractal dimension, and vector dispersion from coral reef 3D models. *PLoS One* **12**, 1–18. <https://doi.org/10.1371/journal.pone.0175341>

## Supporting Information

Additional supporting information may be found online in the Supporting Information section at the end of the article.

**Figure S1.** 3D textured meshes of Sab-1, Sab-3 and Sab-4 hummocks over the whole sampling period (from 3rd of December 2016 to 31st of December 2017).

**Figure S2.** Annual variation of sea state conditions according to mean daily values of the Douglas scale.

**Figure S3.** Measurement of the density of worm tubes with virtual 10 × 10 cm frames.

**Figure S4.** Accuracy of 3D models of pebbles used for testing proportional accuracy and to assess procedural errors expressed in terms of linear length and volume.

**Figure S5.** Correlation matrix of model-based surface complexity metrics (3D surface complexity or  $SurfC_{[3D]}$  and virtual “chain-and-tape” method for the estimation of averaged linear rugosity or  $LR_{[3D]}$ ) against *in-situ* traditional “chain-and-tape” measurements ( $LR_{[chain]}$ )

**Figure S6.** Box plots of volumetric change over the whole sampling period of *Sabellaria* hummocks.

**Figure S7.** Fitting results of the Bayesian model to investigate the effects of sea state (Douglas scale) at colony-level on the main *Sabellaria* metrics extracted from 3D models.

**Figure S8.** Residual variance per colony from the Bayesian model to investigate the effects of sea state (Douglas scale) on the main *Sabellaria* metrics extracted from 3D models and their 95% credibility intervals.